

03,10,16

Investigation of the doping level of semiconductor nanowires via Raman spectroscopy

© V.A. Sharov^{1,2}, P.A. Alekseev¹, V.V. Fedorov², I.S. Mukhin²

¹ Ioffe Institute,
St. Petersburg, Russia

² Alferov Academic University, RAS,
St. Petersburg, Russia

E-mail: vl.sharov@mail.ru

Received January 16 2025

Revised February 14, 2025

Accepted February 22, 2025

The development of characterization techniques for the doping level measurements of epitaxial semiconductor nanowires is an important task on the way to their industrial implementation. In this paper, a method for the doping level measurement using Raman spectroscopy is proposed. The Raman spectra of single vertical gallium phosphide nanowires from a series of samples with different doping levels and types are analyzed. The relationship between the intensity and width of the longitudinal optical phonon mode with the nanowire doping level caused by the phonon-plasmon interaction, is shown.

Keywords: GaP, nanowires, doping, Raman scattering, plasmon-phonon interaction, molecular beam epitaxy.

DOI: 10.61011/PSS.2025.03.61057.11-25

Introduction

Semiconductor nanowires (NWs) are quasi-one-dimensional nanostructures that feature high aspect ratio, typical length of several microns and diameter from tens to hundreds nanometers. Due to high surface-to-volume ratio, NWs have a number of advantages compared with planar structures. The advantages include: defect-free epitaxial growth of lattice-unmatched heterostructures, including monolithic integration of optoelectronic materials on silicon substrates [1]; synthesis of arsenides and phosphides with purely zinc blende and wurtzite crystal structure [2]; combination of wurtzite and zinc blende phases with a limiting case in the form of quantum dots of one phase in the matrix of the other phase [3]. all this drives the interest in the development of NWs growth technology and implementation of NWs-based semiconductor devices — solar cells, waveguides, light-emitting diodes, lasers, single photon sources [4]. Controlled doping is currently an important task on the way towards the device implementation of NWs [5]. Development of highly doped NWs growth modes, post-growth methods for testing the doping level and its spatial distribution is necessary for reproducible synthesis p – n of heterojunctions with preset parameters. This study investigates the ability to determine the doping level of GaP NWs by Raman scattering (RS) spectra. RS spectroscopy method was used to examine NWs of 5 arrays grown in different thermodynamic conditions and doping impurity fluxes. Spectrum shape was analyzed within the plasmon-phonon interaction model, relation between the doping level and LO mode intensity was established.

1. Results

The studied NWs arrays were grown by the molecular-beam epitaxy method on (111) silicon substrates in a self-catalytic mode. Synthesis was carried out in the Veeco Gen III system, beryllium and silicon were used as p - and n -type dopants.

Five GaP NWs samples were examined, SEM images of the corresponding arrays are shown in the insets in Figure 1. Samples No. 1–2 were grown without dopants (Sample No. 1: growth temperature $T = 610^\circ\text{C}$, flux ratio of groups V and III $V/\text{III} = 18$, Si and Be flux is cut off; sample No. 2: $T = 630^\circ\text{C}$, $V/\text{III} = 24$, Si and Be is cut off) Samples No. 3, 5 were grown with Be flux in different thermodynamic conditions (Sample No. 3: $T = 680^\circ\text{C}$, $V/\text{III} = 12$, Be source temperature $T_{\text{Be}} = 680^\circ\text{C}$; sample No. 5: $T = 640^\circ\text{C}$, $V/\text{III} = 20$, $T_{\text{Be}} = 680^\circ\text{C}$). Sample No. 4 was obtained by means of two-stage growth: first a core was grown without a dopant flux using the vapor–liquid–solid (VLS) process, then the gallium flux was stopped and, thus, the catalytic drop disappeared. Then, a GaP shell was formed around the core in the vapor–solid (VS) with turned on silicon flux. Growth conditions of sample No. 4 at each stage are detailed in [8].

Previously in [6–8], an independent evaluation of the doping level was made for NWs from of the studied arrays using current-voltage curves measured on single vertical crystals by conductive atomic-force microscopy. thus, background doping of NWs from sample No. 1 was evaluated at level $N_A = 1 \cdot 10^{16} \text{ cm}^{-3}$ [6]. The same evaluation is also valid for sample No. 2 due to the identical growth conditions. Work [7] provides a current-voltage curve of NWs from sample No. 3, this curve suggests

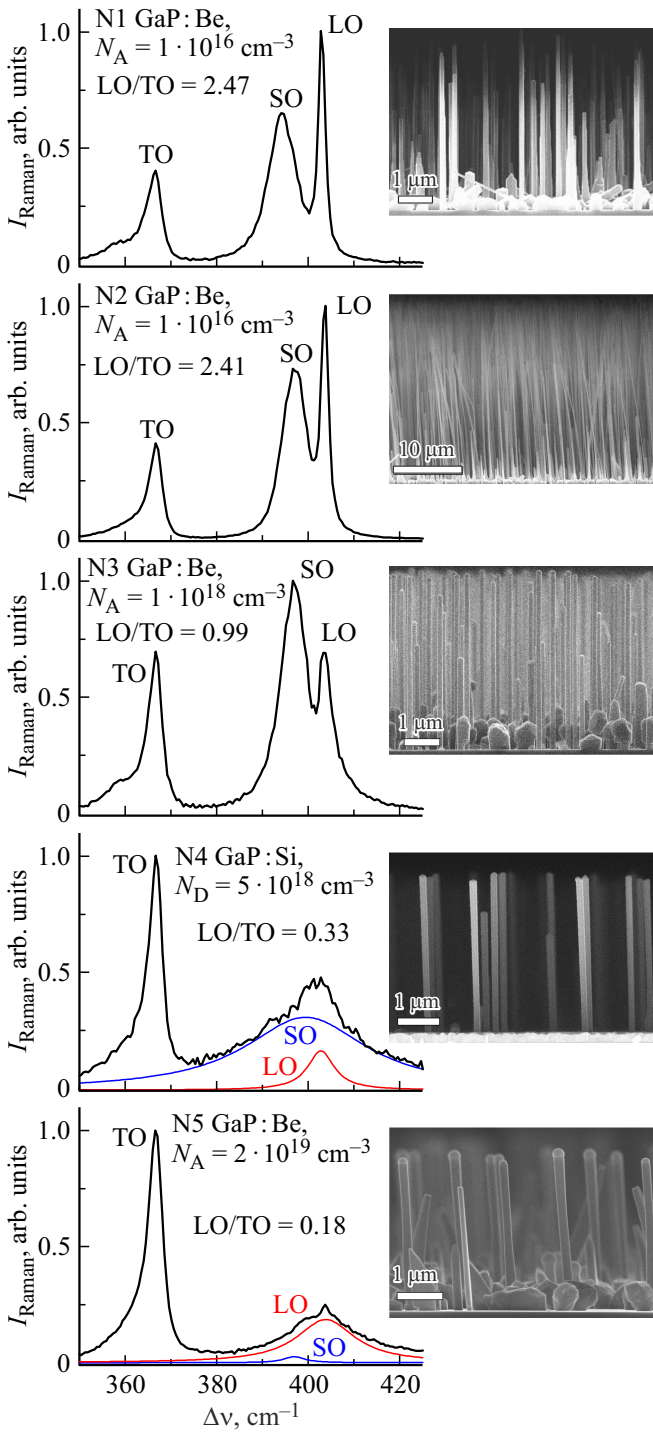


Figure 1. rs spectra of single vertical gap NWs with different doping levels. The insets show SEM images of NWs arrays.

that the doping level is not higher than $N_A = 1 \cdot 10^{18} \text{ cm}^{-3}$. Study [8] analyzed the conductivity of individual NWs from arrays No. 4 and 5 and concentration of free carriers was evaluated at $N_D = 5 \cdot 10^{18} \text{ cm}^{-3}$ and $N_A = 2 \cdot 10^{19} \text{ cm}^{-3}$, respectively.

RS spectra were measured using the Horiba LabRam HR800 system equipped by 532 nm solid-state laser, $\times 100$

lens (N.A. = 0.9), and a piezoelectric scanner allowing spatial mapping of the RS signal with a nanometer accuracy of pumping spot positioning. The experiment was performed in the backscattering configuration, the excitation wave vector was oriented along the vertical NWs axis. Figure 1 shows typical rs spectra from single vertical NWs from samples No. 1–5. Spectra were measured by recording 2d maps of the rs signal in a random $3 \times 3 \mu\text{m}^2$ region at 300 nm steps, then points with the highest integral intensity and corresponding to coincidence of the NWs axis and optical lens axis were chosen from these maps. During mapping, the lens was focused on the NWs tips, thus, avoiding the contribution to spectra from the substrate and spurious GaP layer. The spectra are normalized from 0 to 1 for perception convenience. They contain 3 RS modes: transverse optical (TO), surface optical (SO) and longitudinal optical (LO) modes. On samples No. 2–3, these modes are located at 366, 397 and 403 cm^{-1} , which corresponds to the literature data for gap NWs [9,10]. Sample No. 1 has SO and LO shifts at 394 and 402 cm^{-1} , respectively, that might be attributed to the presence of the wurtzite phase as reported in [6]. Intensity ratio of LO and TO modes (LO/TO), that correlates with the expected NWs doping level, is of interest. Thus, for low doped samples No. 1–2, this ratio is 2.47 and 2.41, respectively, for sample No. 3 moderately beryllium-doped — the ratio is 0.99, for samples No. 4–5 highly beryllium- and silicon-doped — the ratio is 0.33 and 0.18, respectively. Samples No. 4–5 also have pronounced decay and broadening of SO and LO, their Lorentz decomposition is shown with colored lines in Figure 1 for convenience.

Observed decay and broadening of the LO peak with increasing doping level might be associated with the phonon-plasmon interaction. The same effect was previously observed in NWs *n*-GaAs and *p*-GaAs [11,12], well as in highly alloyed *p*-GaAs substrates [13]. Raman scattering from combined plasmon-LO phonon mode results from optical polarizability modulation due to atomic shifts and macroscopic longitudinal electric field. Raman scattering of the Stokes LO peak depending on the frequency ω in the presence of phonon-plasmon interaction can be written as [12]:

$$I_s(\omega) = \frac{A\omega\Gamma_p\omega_p^2[\omega_{\text{TO}}^2(1+C) - \omega^2]}{D}, \quad (1)$$

$$D = [\omega^2(\omega_{\text{LO}}^2 - \omega^2) - \omega_p^2(\omega_{\text{TO}}^2 - \omega^2) + \gamma\Gamma_p\omega^2]^2 + [\Gamma_p\omega(\omega_{\text{LO}}^2 - \omega^2) + \gamma\omega(\omega_p^2 - \omega^2)]^2. \quad (2)$$

Here, A is the constant, $\omega_{\text{LO,TO}}$ are longitudinal and transverse optical phonon frequencies, C is the Faust–Henry coefficient, that is equal to -0.51 in gallium phosphide [14], γ is the LO mode decay constant, ω_p is the plasma frequency, Γ_p is the plasma decay constant, m^* is the effective mass:

$$\omega_p^2 = \frac{pe^2}{\epsilon_\infty\epsilon_0m^*}, \quad \Gamma_p = \frac{e}{\mu m^*},$$

Comparison of carrier concentrations measured by the conductive AFM and RS spectroscopy methods

	Doping level, N, cm^{-3}				
	No. 1	No. 2	No. 3	No. 4	No. 5
Conductive AFM	$1 \cdot 10^{16}$ [6]	$1 \cdot 10^{16}$ [6]	$1 \cdot 10^{18}$ [7]	$5 \cdot 10^{18}$ [8]	$2 \cdot 10^{19}$ [8]
RS spectroscopy	$5 \cdot 10^{17}$	$5 \cdot 10^{17}$	$1.6 \cdot 10^{18}$	$6.2 \cdot 10^{18}$	$0.8 \cdot 10^{19}$

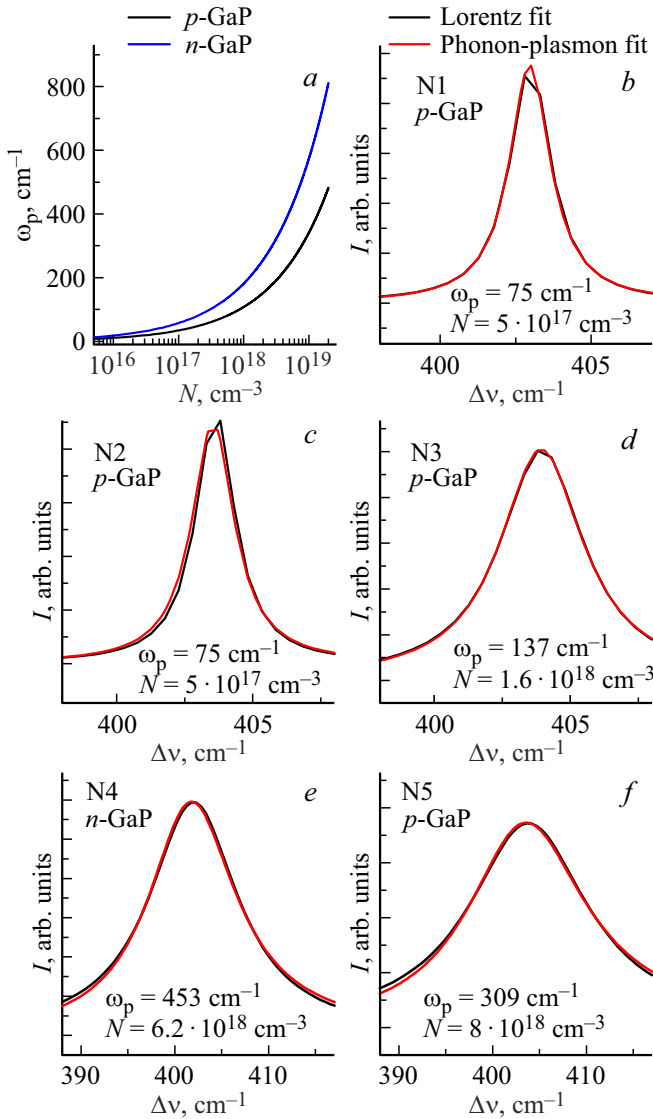


Figure 2. (a) Dependence of the plasma frequency on the doping level for n - and p -GaP; (b–f) Lorentz functions corresponding to the experimental Raman LO modes from NWs from samples No. 1–5 (black curves) and corresponding phonon-plasmon modes calculated using equation 1 (red curves).

$$m_e^* = \left[\frac{1}{3} \left(\frac{2}{m_t} + \frac{1}{m_l} \right) \right]^{-1}, \quad m_h^* = \frac{m_{lh}^{*3/2} + m_{hh}^{*3/2}}{m_{lh}^{*1/2} + m_{hh}^{*1/2}}. \quad (3)$$

LO components of the spectra shown in Figure 1 were simulated using equations (1)–(3). The following fixed

values were used for the calculations: $C = -0.51$ [14], $\mu_e = \mu_h = 10 \text{ cm}^2/(\text{B} \cdot \text{c})$, $m_t = 0.22m_0$, $m_l = 1.12m_0$, $m_{lh} = 0.14m_0$, $m_{hh} = 0.79m_0$, $m_e^* = 0.3m_0$, $m_h^* = 0.85m_0$, $\Gamma_p^{n\text{-GaP}} = 3110 \text{ cm}^{-1}$, $\Gamma_p^{p\text{-GaP}} = 1100 \text{ cm}^{-1}$, $\gamma = 1.1$ [15], plasma frequency ω_p varied freely. Figure 2, a shows the dependence of ω_p on the concentration of free carriers N in n - and p -GaP (blue and black curves, respectively). Then Figure 2, b–f shows the LO mode simulation data for five samples: simulated peaks (red curves) plotted by varying ω_p to achieve the best coincidence with the experiment were overlaid on the experimental data (black curves). The found values of ω_p were used to calculate the concentrations of free carriers that are also shown in Figure 2.

The table shows comparison of the doping levels of samples No. 1–5 measured in [6–8] using conductive AFM with RS spectroscopy data. It is fair to say that evaluations made by the two methods agree with each other. A minor difference may be due to doping dispersion within a single array. At the same time, for sample No. 1–2, the RS spectra appear to be slightly overestimated, which may be associated with the growth of carrier mobility at low doping levels that was not included in simulation.

2. Conclusion

Raman scattering spectra from single GaP nanowires from 5 arrays with different doping levels and types were studied. It was shown that the LO mode undergoes decay and broadening with high doping of NWs irrespective of the doping type, which is explained in terms of the phonon-plasmon interaction model. The measured spectra were used to evaluate the NWs doping level and the evaluation data was in agreement with the previous atomic-force microscopy results. Thus, the RS spectra may be used as an additional tool for determining the NWs doping level.

Funding

The study was supported by grant provided by the Russian Science Foundation No. 23-72-01082, <https://rscf.ru/project/23-72-01082/>.

Conflict of interest

The authors declare no conflict of interest.

References

- [1] A. Bolshakov, V. Fedorov, K.Y. Shugurov, A. Mozharov, G. Sapunov, I. Shtrom, M. Mukhin, A. Uvarov, G. Cirlin, I. Mukhin. *Nanotechnology* **30**, 39, 395602 (2019).
- [2] H.J. Joyce, J. Wong-Leung, Q. Gao, H.H. Tan, C. Jagadish. *Nano letters* **10**, 3, 908 (2010).
- [3] N. Akopian, G. Patriarche, L. Liu, J.-C. Harmand, V. Zwiller. *Nano letters* **10**, 4, 1198 (2010).
- [4] L.N. Quan, J. Kang, C.-Z. Ning, P. Yang. *Chem. Rev.* **119**, 15, 9153 (2019).
- [5] W. Kim, L. Güniat, A. Fontcuberta, I. Morral, V. Piazza. *Appl. Phys. Rev.* **8**, 1, 011304 (2021).
- [6] V. Sharov, P. Alekseev, V. Fedorov, M. Nestoklon, A. Ankudinov, D. Kirilenko, G. Sapunov, O. Koval, G. Cirlin, A. Bolshakov. *Appl. Surf. Sci.* **563**, 150018 (2021).
- [7] V. Sharov, P. Alekseev, V. Fedorov, I. Mukhin. (IOP Publishing, 2021) Vol. 2086 p. 012207.
- [8] V. Sharov, K. Novikova, A. Mozharov, V. Fedorov, D. Kirilenko, P. Alekseev, I. Mukhin. *Scripta Materialia* **248**, 116128 (2024).
- [9] R. Gupta, Q. Xiong, G. Mahan, P. Eklund. *Nano Lett.* **3**, 12, 1745 (2003).
- [10] V.A. Sharov, A.M. Mozharov, V.V. Fedorov, A. Bogdanov, P.A. Alekseev, I.S. Mukhin. *Nano letters* **22**, 23, 9523 (2022).
- [11] B. Ketterer, E. Uccelli, A.F. i Morral. *Nanoscale* **4**, 5, 1789 (2012).
- [12] N.I. Goktas, E.M. Fiordaliso, R. LaPierre. *Nanotechnology* **29**, 23, 234001 (2018).
- [13] A. Mlayah, R. Carles, G. Landa, E. Bedel, A. Muñoz-Yagüe. *J. of Appl. Phys.* **69**, 7, 4064 (1991).
- [14] C. Flytzanis. *Phys. Rev. Lett.* **23**, 23, 1336 (1969).
- [15] D. Lockwood, G. Yu. N. Rowell. *Solid State Commun.* **136**, 7, 404 (2005).

Translated by E.Ilinskaya